Application of Electrical Impedance Tomography in Pulp Flow Measurement

Shaomin Zhou, Jouko Halttunen
(Institute of Measurement and Information Technology, Tampere University of Technology,
Box 692, 33101 Tampere, Finland)

Abstract Electrical impedance tomography is an imaging method that can profile the resistivity distribution within a domain using a non-invasive sensor. It is a promising method for multiphase flow measurement. This paper describes an EIT system for monitoring the consistency, air bubbles and velocity in pulp flow.

Keywords: EIT; Multiphase Flow; Cross correlation

1. Introduction

In industrial application, the measurement of multiphase flow is very important, but it is difficult to solve due to the complex behavior inside the flow. Process Tomography technique provides a new method to visualize the internal behavior in industrial process, for example, the gas/liquid, gas/solid and the other multiphase flow. On the other hand, electrical impedance tomography (EIT) is based on the principle of electrical impedance sensitivity; it has several advantages over the other traditional means, such as the non-invasive sensor, lack of radiation, rapid response. Therefore, it has been widely developing in recent years.

EIT images offer the distribution information about each phase in a multiphase flow, in order to calculate the mass flow or volume flow, the velocity of the flow must be measured. Several solutions have been developed for this purpose, such as applying cross correlation technique or using a traditional velocity meter to obtain the velocity information.

This paper describes a flow measurement system based on process tomography technique and cross correlation technique. This system will be applied to measure the pulp flow.

2. Measurement principle

The basic idea is to apply the process tomography to obtain the images containing the distribution information about each phase and calculate the cross correlation of the images to get the velocity information, then the volume flow or mass flow can be calculated.

2.1 Physical model of EIT

EIT is an imaging method that can profile the resistivity distribution within a domain. If each phase in the flow has different conductivity, it is possible to identify them by the resistivity measurements.

Fig. 1 shows the physical model of EIT. A set of electrodes are installed around the pipe or vessel to be imaged. The distribution function of conductivity is σ. A current is injected via a pair of electrodes and the response voltages are measured from the other electrodes. The response voltages depend on the position of the component boundaries within their sensing zones.

The underlying relationships, which govern the interaction of electricity and magnetism, are summarized by Poisson equation:

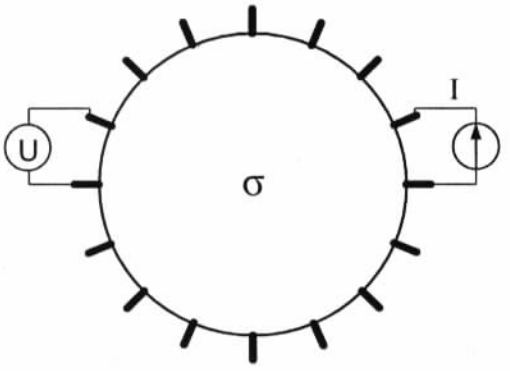

Fig. 1 Physical mode of EIT.

$$\nabla \cdot (\sigma \nabla u) = 0 \tag{1}$$

where

σ is the distribution function of conductivity

u is the distribution of potential

Because the relationship between σ and u is nonlinear, it is very difficult to obtain analytic solution of Eqn. (1). Therefore, the numerical method is applied to get an approximate solution.

2.2 Image reconstruction algorithm

The reconstruction problem is to obtain an approximation to the conductivity distribution in the interior from the boundary measurements. This problem is challenging because it is not only nonlinear, but also ill posed, which means that large changes in the interior can correspond to very small changes in the measured data.

From a theoretical point of view, all possible boundary measurements do uniquely determine the conductivity in the interior.[1][2][3] However, in practice we are limited to a finite number of electrodes and a finite number of current patterns.

Many reconstruction algorithms have been proposed. Cheney et al.[4] classified approaches into several categories. The first are based on linear approximations. These are noniterative methods based on the assumption that the conductivity does not differ very much from a constant. Examples of linear methods are the Barber-Brown backprojection method[5] and related methods,[6][7] Calderon's approach,[8][9][10] moment methods,[11][12] and one-step Newton methods.[13]

The modified Newton-Raphsom algorithm[14] is common used in EIT. This method implements a FEM solver and iterative method to compute the conductivity distribution. A forward transform **F** to describe the relationship between the boundary voltages **V** and the resistivity **r** is given by:

$$\mathbf{V} = \mathbf{F}(\mathbf{r}) \tag{2}$$

The quadratic error $\mathbf{e}(\mathbf{r})$ between the computed voltages of the previous equation and the measured voltages $\mathbf{V}_0$ is defined by:

$$\mathbf{e}(\mathbf{r}) = \frac{1}{2}\left[\mathbf{F}(\mathbf{r}) - \mathbf{V}_0\right]^T \left[\mathbf{F}(\mathbf{r}) - \mathbf{V}_0\right] \tag{3}$$

Here T represents the matrix transpose. Minimization of this error with respect to the resistivity gives:

$$\mathbf{e}'(\mathbf{r}) = \left[\mathbf{F}'(\mathbf{r})\right]^T \left[\mathbf{F}(\mathbf{r}) - \mathbf{V}_0\right] = 0 \tag{4}$$

where $\mathbf{F}'(\mathbf{r})$ is the Jacobian matrix.

$$\left[\mathbf{F}'(\mathbf{r})\right]_{ij} = \frac{\partial \mathbf{F}_i}{\partial \mathbf{r}_j} = \begin{pmatrix} \frac{\partial F_1}{\partial r_1} & \frac{\partial F_1}{\partial r_2} & \cdots & \frac{\partial F_1}{\partial r_n} \\ \frac{\partial F_2}{\partial r_1} & \frac{\partial F_2}{\partial r_2} & \cdots & \frac{\partial F_2}{\partial r_n} \\ \vdots & \vdots & \vdots & \vdots \\ \frac{\partial F_m}{\partial r_1} & \frac{\partial F_m}{\partial r_2} & \cdots & \frac{\partial F_m}{\partial r_n} \end{pmatrix} \tag{5}$$

Finding the Taylor expansion of Eqn. (4) and ignoring the non-linear terms, Yorkey et al.[14] obtained a correction factor for the conductivity at the k^{th} iteration as:

$$\Delta \mathbf{r}^k = -\left\{\left[\mathbf{F}'(\mathbf{r}^k)\right]^T \mathbf{F}'(\mathbf{r}^k)\right\}^{-1} \left[\mathbf{F}'(\mathbf{r}^k)\right]^T \left[\mathbf{F}(\mathbf{r}^k) - \mathbf{V}_0\right] \tag{6}$$

The updated conductivity distribution becomes:

$$\mathbf{r}^{k+1} = \mathbf{r}^k + \Delta \mathbf{r}^k \tag{7}$$

The Jacobian is recalculated at each iteration and thus

an efficient FEM implementation is required to compute the forward transformation and Jacobian. The principle problem associated with this algorithm however, is the inversion of the matrix:

$$\mathbf{A} = \left[\mathbf{F}'(\mathbf{r}^k)\right]^T \mathbf{F}'(\mathbf{r}^k) \tag{8}$$

This matrix **A** is often ill-conditioned and thus regularization techniques are required if images are to be reconstructed from real data which will inevitably include measurement noise. Yorkey et al. implemented the Marquardt method to achieve the regularization[14], whilst Hua et al. modified the term to be minimized Eqn. (3),[15] by adding a penalty term such that:

$$\mathbf{e}(\mathbf{r}) = \frac{1}{2}\left[\mathbf{F}(\mathbf{r}) - \mathbf{V}_0\right]^T \left[\mathbf{F}(\mathbf{r}) - \mathbf{V}_0\right] + \lambda \mathbf{r}^T \mathbf{P}\mathbf{r} \tag{9}$$

where λ is a scalar and **P** is a positive definite matrix, depending on the form of prior information. Generally, **P** can be a simple diagonal matrix. The correction factor in Eqn. (6) becomes:

$$\begin{aligned}\Delta \mathbf{r}^k = -\left\{\left[\mathbf{F}'(\mathbf{r}^k)\right]^T \mathbf{F}'(\mathbf{r}^k) + 2\lambda \mathbf{P}\right\}^{-1} \\ \left[\mathbf{F}'(\mathbf{r}^k)\right]^T \left[\mathbf{F}(\mathbf{r}^k) - \mathbf{V}_0\right]\end{aligned} \tag{10}$$

The matrix **A** now includes an additional term and this tends to improve the matrix condition. However, the value of these regularization terms can greatly alter the performance of the algorithm. If λ is too high, the smoothing may result in severely degraded image resolution, whilst a small λ will have little effect on the conditioning of the matrix.

Newton-Raphson algorithm can be divided into two sections: the forward problem and inverse problem. The forward problem can be described as finding the voltage distribution within the region, given knowledge of the conductivity distribution and the specification of the boundary conditions. Image reconstruction is an example of an inverse problem, in which we try to recover the conductivity distribution from the boundary measurements. Except under highly constrained circumstances, a single set of boundary measurements will not convey sufficient information to uniquely determine the conductivity distribution. To reconstruct an image, the application of a number of independent measurement sets is required.

The inverse problem therefore becomes one of finding a conductivity distribution which is consistent with all the measurement data sets and any particular constraints which can be applied. In general, as more independent measurements are made, the ability to reconstruct a greater number of independent conductivity elements will increase. However, this improvement in spatial resolution is not only determined by the number of independent measurements, but is also related to measurement accuracy and noise,[16] and to the applied current patterns and voltage measurement configurations.[17]

2.3 Flow velocity measurement

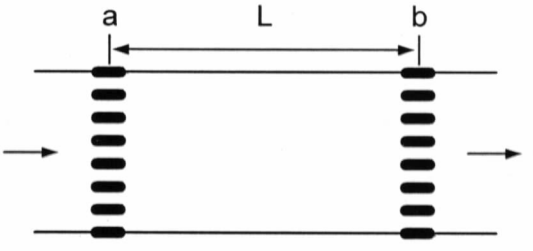

Fig. 2 Model of dual 16-electrode sensor.

In this research, the velocity was measured by pixel-pixel cross correlation. Fig. 2 shows a dual 16-electrode sensor for this system. The cross section was divided into 16 pixels (see Fig. 3). If the flow pattern can be considered 'frozen' during passing from plane A to plane B, the time that the k^{th} pixel moves from plane A to plane B can be determined by following cross-correlation function:

$$\begin{aligned}R_k(j) = \frac{1}{N}\sum_{i=1}^{N} x_k(i) y_k(i+j) \\ j = 0,1,2,\ldots,M \quad k = 1,2,\ldots,16\end{aligned} \tag{11}$$

where $x_k(i)$ and $y_k(i)$ are the up-stream and down-stream signals, N is the number of samples in cross correlation calculation, j is the number of delayed samples, and k is the pixel index. When the

time delay equals to the flow transit time τ^*, the cross correlation function produces the maximum value. The flow velocity can be calculated $V=L/\tau^*$, where L is the distance between the sensors. In total, 16 velocities can be calculated.

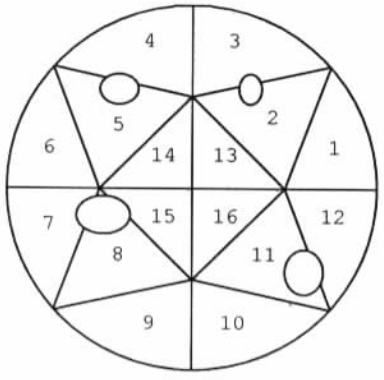

Fig. 3 16 pixels in cross section.

After the fraction profile and the velocity profile have been obtained, the volumetric flowrate can be derived:

$$Q = \sum_{i=1}^{m} \beta_i V_i A_i \qquad (12)$$

where A_i is the area of i^{th} pixel, β_i is the modifying factor of flowrate.

3. Measurement system design

The system includes a host computer, two data acquisition system (DAS) and a dual 16-electrode sensor, as shown in Fig. 4.

DAS1 and DAS2 acquire data from the electrodes and send them to the host computer. The host computer reconstructs the images and then calculates flow velocity based on the cross correlation method. The part inside the broken line in Fig. 5 shows the block diagram of DAS.

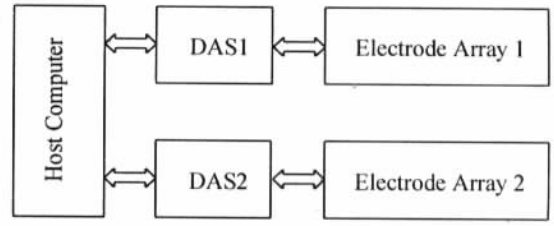

Fig. 4 Structure of system.

The DAS is controlled by a single-chip computer and perform the following functions: measurement, de-modulation and control; waveform generation and synchronization; multiplexer control. The DAS communicates with the host computer via RS232 serial link to receive logging commands and to transfer logged data for subsequent image reconstruction.

Sine wave is generated by EPROM-based function generator. A synchronous signal is also generated for demodulation purpose. The output frequency can be selected among 153 Hz, 200 Hz, 300 Hz ... 19.5 kHz by different factor of frequency divider. The amplitude of the output wave can be adjusted by the reference voltage of DAC. The V/I convertor is a voltage-control current source. Multiplexers switch the electrodes for current injecting and response voltage sampling. Resistivity signal is demodulated by a phase-sensitive demodulator AD630 and digitized by a 12-bit A/D convertor. The single-chip computer accepts commands from host computer to initialize the hardware and sends data to host computer via RS232C. The whole system is simple and flexible.

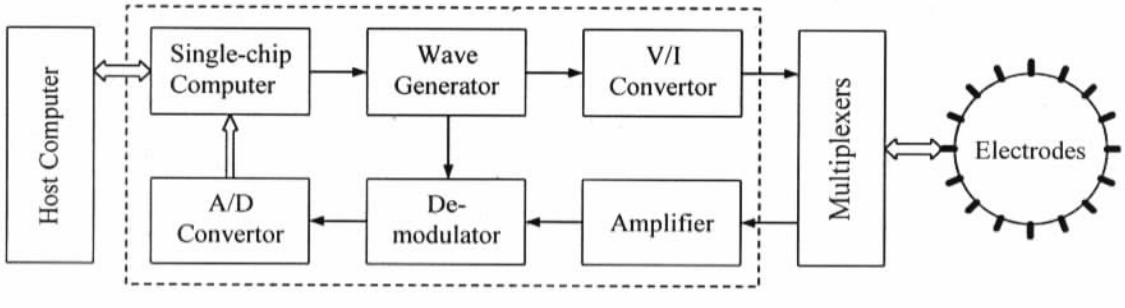

Fig. 5 Block diagram of data acquisition system.

4. Experimental Results

The experiments were carried out in a dual-plane sensor (see Fig. 6). Each plane includes 16 electrodes. For the static experiments, the tank was full of pulp (about 3,5% consistency) and some plastic rods (12 mm and 20 mm diameter) were used to make the conductivity distribution inhomogeneous.

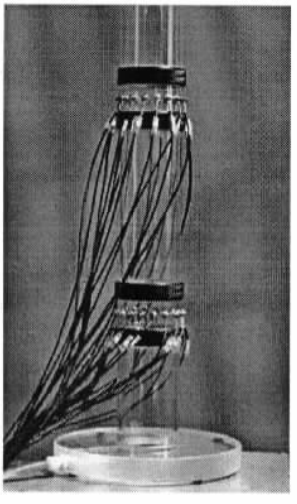

Fig. 6 Dual-plane sensor.

Fig. 7 shows the reconstruction images when the plastic rods in different positions.

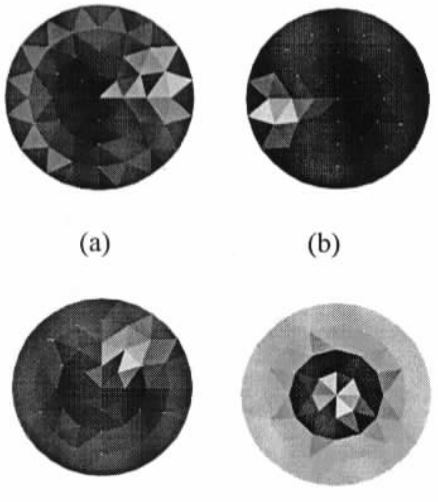

(a) (b)

(c) (d)

Fig. 7 Experimental results. (a) Plastic rod on the right; (b) Rod on the left; (c) Rod near centre; (d) Rod at the centre.

To simulate the flow motion, a plastic rod was put into the tank, and then pulled from the bottom to top. In Fig. 8, the first curve is signal from the 7th pixel in down-plane; the second curve is the signal from the 7th pixel in up-plane and the third curve is the cross correlation curve.

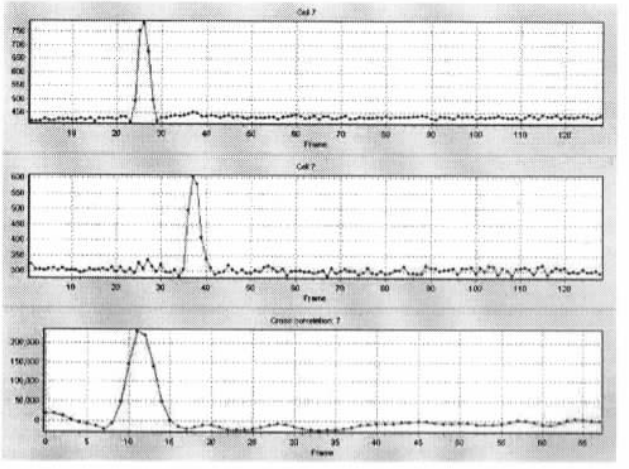

Fig. 8 Velocity measurement by cross correlation method.

5. Summary

Process tomography provides a novel method for multiphase flow measurement, including solids fraction profile, flow regime, velocity profile and volumetric flowrate. As our first stage, we created a simple and low cost flow measurement system. The two independent data acquisition systems give a flexible solution for the measurement system. The host computer reconstructs images, calculates cross correlation function and parameters of flow. At the same time, the two data acquisition systems acquire data from electrode arrays. In order to realize online measurement, the real-time performance of DAS needs to be improved further.

Acknowledgment

The financial support of the National Technology Agency of Finland (TEKES) and Paper Manufacturer Graduate School (PMGS) are gratefully acknowledged.

References

[1] Kohn R. and Vogelius M. Determining conductivity by boundary measurements. *Comm. Pure Appl. Math.*, 1984, 37: 113 – 123.

[2] Sylvester J. and Uhlmann G.. A uniqueness theorem for an inverse boundary value problem in electrical prospection. *Comm. Pure Appl. Math.*, 1986, 39: 91 – 112.

[3] Nachman A.I. Reconstruction from boundary measurements. *Ann. of Math.*, 1988, 128: 531 – 576.

[4] Cheney M., Isaacson D, Newell J.C. Electrical Impedance Tomography. *SIAM Review*, 1999, 41: 85 – 101

[5] Barber D.C. and Brown B.H. Applied Potential Tomography (Review Article). *J. Phys. E:Sci. Instrum*, 1984, 17: 723 – 733.

[6] Santosa F. and Vogelius M. A backprojection algorithm for electrical impedance imaging. *SIAM J. Appl. Math.*, 1990, 50: 216 – 243.

[7] Berenstein C. and Tarabusi E.C. Inversion formulas for the k-dimensional Radon transform in real hyperbolic spaces. *Duke Math. J.*, 1991, 62: 1 – 19.

[8] Calderon A.P. On an inverse boundary value problem. *Seminar on Numerical Analysis and Its Applications to Continuum Physics, Soc. Brasileira de Matematica*, Rio de Janeiro, 1980, 65 – 73.

[9] Isaacson D. and Cheney M. Current problems in impedance imaging. *in Inverse Problems in Partial Differential Equations, D. Colton, R. Ewing, and W. Rundell, eds., SIAM, Philadelphia*, 1990, 141 – 149.

[10] Isaacson D. and Cheney M. Effects of measurement precision and finite numbers of electrodes on linear impedance imaging algorithms. *SIAM J. Appl. Math.*, 1991, 51: 1705 – 1731.

[11] Connolly T.J. and Wall D.J.N. On an inverse problem, with boundary measurements, for the steady state diffusion equation. *Inverse Problems*, 1988, 4: 995 – 1012.

[12] Allers A. and Santosa F. Stability and resolution analysis of a linearized problem in electrical impedance tomography. *Inverse Problems*, 1991, 7: 515 – 533.

[13] Cheney M., Isaacson D., Newell J.C., Simake S. and Goble J. NOSER: An Algorithm for Solving the Inverse Conductivity Problem. *Int. J. Imag. Sys. Technol.*, 1990, 2: 66 – 75.

[14] Yokey T.J., Webster J.G., Tompkins W.J. Comparing Reconstruction Algorithms for Electrical Impedance Tomography. *IEEE Trans. Biomed. Eng.*, 1987, Vol. 11: 843 – 852.

[15] Hua P., Webster J.G. and Tompkins W.J. Iterative Reconstruction Methods Using Regularization and Optimal Current Patterns in Electrical Impedance Tomography. *IEEE Trans. Medical Image.*, 1991, Vol. 10: 624 – 628.

[16] Seagar A.D., Baber D.C. and Brown B.H. Theoretical Limits to Sensitivity and Resolution in Impedance Imaging. *Clin. Phys. Physiol. Meas.*, 1987, 8 (Suppl. A): 13 – 31.

[17] Avis N.J. and Barber D.C. Image Reconstruction Using Non-Adjacent DriveConfigurations. *Physiol. Meas.*, 1994, 15 (Suppl. 2A): 153 – 160.